Crack monitoring in concrete beams under bending using ultrasonic waves and coda wave interferometry: the effect of excitation frequency on coda

Journal of Physics: Conference Series **2647** (2024) 182004 doi:10.1088/1742-6596/2647/18/182004

Crack monitoring in concrete beams under bending using ultrasonic waves and coda wave interferometry: the effect of excitation frequency on coda

M Knak[1,3], E Wojtczak[1] and M Rucka[1,2]

[1] Department of Mechanics of Materials and Structures, Faculty of Civil and Environmental Engineering, Gdańsk University of Technology, Narutowicza 11/12, 80-233, Gdańsk, Poland
[2] EkoTech Center, Gdańsk University of Technology, Narutowicza 11/12, 80-233 Gdańsk, Poland
[3] Author to whom any correspondence should be addressed.

magdalena.knak@pg.edu.pl

Abstract. Concrete is one of the most widely used construction materials in the world. In recent years, various non-destructive testing (NDT) and structural health monitoring (SHM) techniques have been investigated to improve the safety and control of the current condition of concrete structures. This study focuses on micro-crack monitoring in concrete beams. The experimental analysis was carried out on concrete elements subjected to three-point bending in a testing machine under monotonic quasi-static loading. During the tests, the fracture process was characterized using ultrasonic waves. The recorded signals were further processed by coda wave interferometry (CWI). This technique allowed the detection of cracks using the decorrelation between ultrasonic wave signals collected at different stages of degradation. Different values of excitation frequencies in the range from 100 kHz to 400 kHz were used to investigate the influence of frequency selection on the effectiveness of the damage indication based on the decorrelation of coda waves. The results obtained from the experiments were intended to highlight the effect of the applied frequencies on the coda wave interferometry.

1. Introduction

Concrete elements such as beams are widely used in engineering structures. Inspection of their condition is an integral part of maintaining the safety of use. Since concrete is a brittle material and has a random, heterogeneous, multi-phase structure, it is very susceptible to cracking. Therefore, the detection of cracks at the earliest possible stage is of great importance. Structural monitoring is one of the most intensively studied fields by researchers. Specifically, great attention is paid to tests that do not interfere with the structure of the object, and thus are related to non-destructive testing (NDT) and structural health monitoring (SHM).

One of the basic and most widely used monitoring approaches is the method using ultrasounds, i.e., ultrasonic testing (UT). It is based on passing ultrasonic waves through the tested object. By using specific sensors, e.g., piezoelectric, it is possible to record output signals which, after appropriate processing, can provide detailed information about the condition of the object. Much work has been done on this subject, particularly under laboratory conditions [1–4].

One of the more advanced methods of processing ultrasonic signals is coda wave interferometry (CWI). Adopted from seismology, CWI has been also used with increasing success in structural diagnostics. Based on ultrasonic measurements at various damage stages of an object, it is possible to detect the changes in its internal structure and even localize the resulting defects. The method is based on comparison-relevant parts of the signals, in which the so-called 'coda' occurs. CWI makes it possible to observe subtle changes in the signal indicating the emerging micro-cracks. The fundamental indicator describing the differences between the signals is the decorrelation coefficient (DC). To improve the method, some variants of the basic DC including translations or stretching of the perturbed signal are applied [5–7], allowing to obtain even more detailed results. The efficiency of the CWI method is very sensitive to the chosen time intervals as well as wave frequencies [7–10]. With an increasing research interest in the application of this data analysis technique, it is important to analyze new cases and improve calculations.

When developing techniques and procedures for detecting and monitoring micro-cracks, it is important to verify the places of their formation and the time in which they occurred. This possibility can be provided by the digital image correlation (DIC) which is an example of an optical method. The method is based on processing images taken at different levels of load and it enables observation of changes in deformation fields and the degree of development of emerging cracks. In previous works, the digital image correlation method has been successfully combined with other NDT techniques [11–14], allowing for the most accurate description of the condition of the object under mechanical degradation.

The current work is focused on the application of UT and CWI monitoring. Optical tracking of the formed crack was performed using the DIC technique. The selected methods allowed effective fracture characterization and early-stage damage detection. Moreover, the proposed placement of the sensors made it possible to estimate the location of the emerging crack using the coda approach. The results obtained from the experiment were intended to highlight the effect of applied frequencies on the coda wave interferometry.

2. Materials and methods

2.1. Object of research

The objects of the tests were four beams (#1 – #4) with dimensions of 40 × 40 × 160 mm^3 (figure 1a). The specimens were made of concrete, prepared from the following composition: CEM I 42.5R (330 kg/m^3), water (165 kg/m^3), sand 0 – 2 (710 kg/m^3), gravel 2 – 8 (664 kg/m^3), gravel 8 – 16 (500 kg/m^3), and superplasticizer (2.31 kg/m^3).

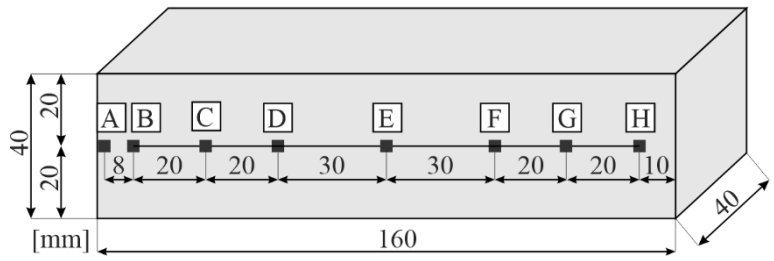

Figure 1. An object of research - specimen geometry.

2.2. Experimental procedure

During the three-point bending tests (performed by Zwick/Roell Z10 universal testing machine – UTM), the fracture process was characterized using DIC and CWI methods (figure 2). The loading was performed with fixed displacement growth equals Δu = 0.05 mm/min. The initial force was set as 20 N. The test stopped after reaching the maximum displacement u_{max} = 0.4 mm, which corresponded to T_{max} = 480 s. The photographs of the samples were taken each 1 s by Aramis Professional set-up.

The front side of the beam has been covered with a suitable random pattern, which made it possible to capture the surface strain field using DIC (figure 2b). The UT monitoring was conducted using a set of PZT transducers attached to the back side of the beam (figure 2b). One of them was an actuator (A) while the others acted as sensors (B – H). The excitation was a wave packet composed of a 5-cycle sine wave modulated by the Hann window. The procedure assumed excitation and registration of wave signals at selected time instances with interval $dT = 1$ s during the whole process of mechanical degradation of concrete specimens in laboratory conditions. The frequencies of input wave signals were set as 100 kHz, 200 kHz, 300 kHz, and 400 kHz for the consecutive samples #1 – #4, respectively. The recorded signals were further processed with a CWI algorithm.

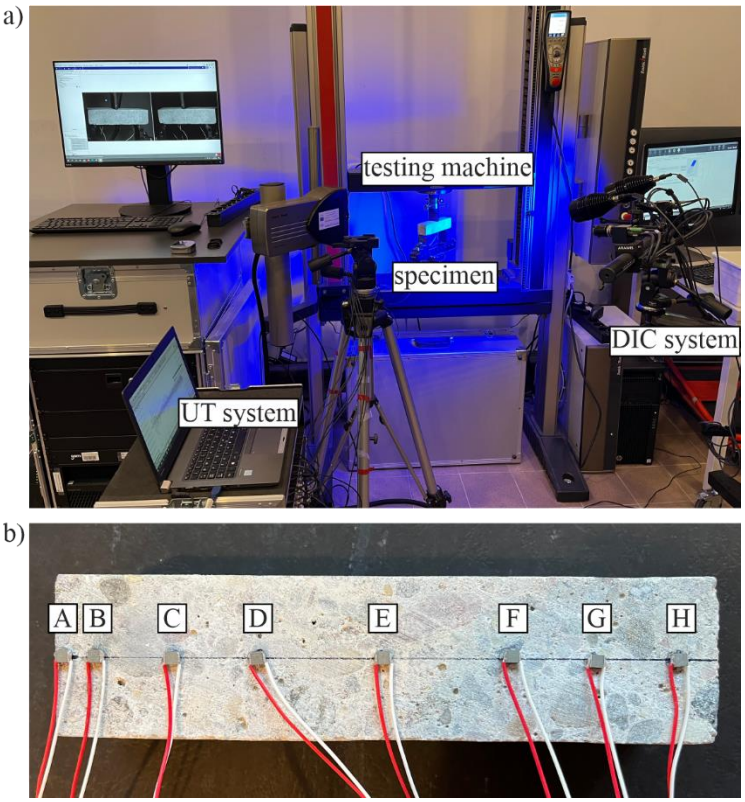

Figure 2. Experimental procedure: a) view of experimental setup, b) photograph of example specimen with location of PZT transducers.

2.3. Coda Wave Interferometry

The ultrasonic signals acquired during the experiment were processed by CWI. The technique allows the detection of weak changes in the medium using the decorrelation between guided wave signals collected at different states. The classical CWI approach compares an unperturbed wave s_i with a perturbed signal s_j, $i,j = 1,2,\ldots,n$. The decorrelation coefficient (DC) is calculated according to equation (1). The main information about slight changes is reflected in the 'tail' of the signal. In a classical approach, all signals in the data are compared to the first one, thus $i = 1$. An important step in performing analysis is accurate time estimation of coda wave occurrence. Subsequently, the main CWI analysis can be done correctly.

$$DC_{i,j} = 1 - \frac{\int_{t_1}^{t_2} s_i(t) \cdot s_j(t) \mathrm{d}t}{\sqrt{\int_{t_1}^{t_2} s_i^2(t) \mathrm{d}t \cdot \int_{t_1}^{t_2} s_j^2(t) \mathrm{d}t}} \tag{1}$$

Another approach is the CWI translation method [5]. $DC(\delta t)$ is calculated following equation (2), where δt is the time shift in a certain time window. The method assumes that the occurring time shift is constant through the whole considered time window. The optimal translation factor should minimize the $DC(\delta t)$ function. In the performed calculations, the signal was shifted in the time domain, where a coefficient selection was made from the range $\delta t = [-5;5] \cdot 10^{-6}$ s with a step $\mathrm{d}\delta t = 5 \cdot 10^{-8}$ s.

$$DC_{i,j}(\delta t) = 1 - \frac{\int_{t_1}^{t_2} s_i(t) \cdot s_j(t + \delta t) \mathrm{d}t}{\sqrt{\int_{t_1}^{t_2} s_i^2(t) \mathrm{d}t \cdot \int_{t_1}^{t_2} s_j^2(t) \mathrm{d}t}} \tag{2}$$

The stretching method is more widely applied in CWI [6,7]. This approach assumes that the perturbed signal is a stretched or compressed version of the reference one. The parameter that determines this change is the stretching factor ε. The $DC(\varepsilon)$ function is calculated according to the following equation (3). To minimize the value of $DC(\varepsilon)$, the stretching factor was selected from a range of $\varepsilon = [-1\%;1\%]$ with a step $\mathrm{d}\varepsilon = 0.001\%$.

$$DC_{i,j}(\varepsilon) = 1 - \frac{\int_{t_1}^{t_2} s_i(t) \cdot s_j\left(t(1+\varepsilon)\right) \mathrm{d}t}{\sqrt{\int_{t_1}^{t_2} s_i^2(t) \mathrm{d}t \cdot \int_{t_1}^{t_2} s_j^2\left(t(1+\varepsilon)\right) \mathrm{d}t}} \tag{3}$$

3. Results and discussion

3.1. Bending test results

The results obtained from three-point bending tests for all samples are presented in figure 3. The load-deflection curves for all beams #1 – #4 have a similar shape and are characterized by a sudden drop in force after the fracture of the samples, as they were made of plain concrete. The load peak values, corresponding times and frequencies are shown in Table 1.

Table 1. The results of bending tests for beams #1 - #4 – peak force values and corresponding times.

	Beam 1	**Beam 2**	**Beam 3**	**Beam 4**
Frequency, f [kHz]	100	200	300	400
Peak force, F_{max} [N]	2644	2495	3189	2942
Corresponding time, T_{peak} [s]	308	282	463	402

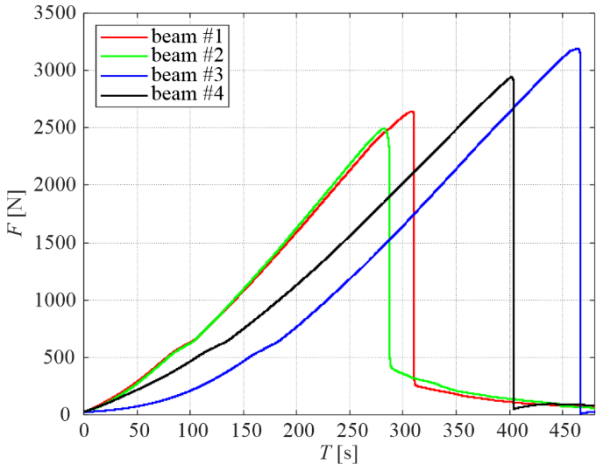

Figure 3. Bending test results: force vs. time diagrams for beams #1 - #4.

3.2. Coda Wave Interferometry Results

The experimental results were evaluated using the procedure of CWI. Firstly, for each beam and sensor, the coda time range was estimated. Each signal was divided into parts with a duration of $dt = 0.01$ ms. The duration of each signal was $t_{max} = 2$ ms. Calculations were conducted according to equation (1). The first signal was taken as a reference one. Figure 4 presents the decorrelation maps for each beam and sensor. The vertical axis T specifies the experiment time and the horizontal axis t refers to the length of the signal. Based on the maps, the corresponding coda occurrence ranges were determined (marked with dashed lines). A solid, horizontal line denotes the peak value occurrence. It can be seen that as the frequency increases, the time range for which the coda is visible decreases. It is the effect of the fact that the higher the frequency, the signals are burdened with a longer tail composed of noise. The determined ranges which were used for further calculations are listed in Table 2 (t_1 and t_2 denote the start and end points of the coda time window, respectively).

Table 2. Coda wave occurrence ranges.

	Beam 1	**Beam 2**	**Beam 3**	**Beam 4**
Sensor	t_1 - t_2 [ms]			
B	0.1 – 1.4	0.2 – 0.8	0.2 – 0.5	0.2 – 0.5
C	0.3 – 2.0	0.5 – 1.5	0.3 – 1.0	0.2 – 0.9
D	0.2 – 2.0	0.5 – 1.5	0.5 – 1.0	0.3 – 0.9
E	0.3 – 2.0	0.3 – 1.5	0.0 – 1.0	0.1 – 0.7
F	0.1 – 2.0	0.2 – 1.5	0.0 – 1.0	0.0 – 0.6
G	0.5 – 2.0	0.5 – 1.5	0.0 – 0.9	0.1 – 0.7
H	0.3 – 2.0	0.3 – 1.5	0.1 – 1.0	0.0 – 0.8

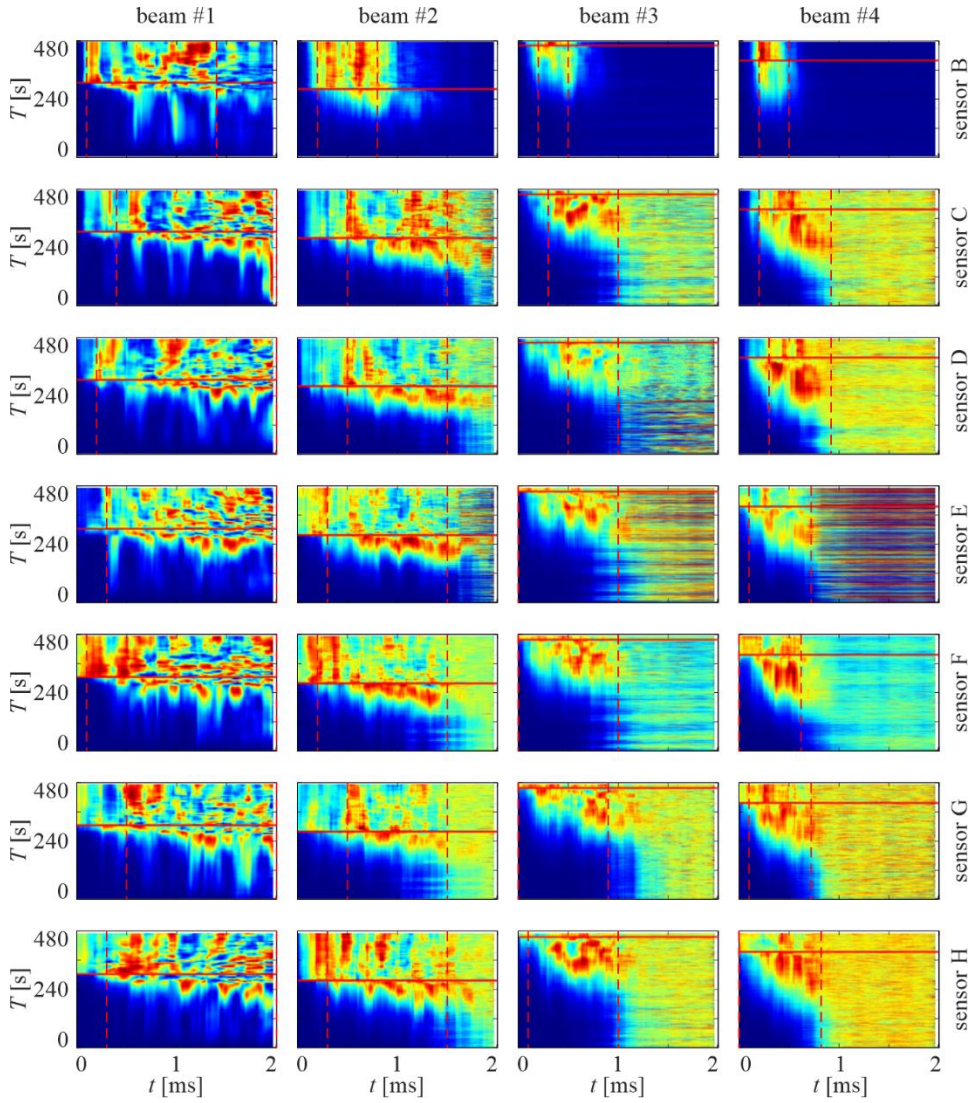

Figure 4. Detection of time range of coda waves for beams #1 - #4 and all sensors.

In the next step, the calculations of *DC*, *DC*(δt) and *DC*(ε) were performed according to equations (1) – (3). Figure 5 shows the changes in decorrelation during the bending test (the values are normalized to unity). In the graph, vertical lines correspond to the maximum load. For each beam, three diagrams were prepared which correspond to the used decorrelation methods. It can be seen that regardless of the calculation method all the *DC* curves exhibit similar behaviour. The first stage of loading is related to a slight growth of *DC*. In this phase, there is no visible defect of the beam structure. During the occurrence of micro-cracks, the *DC* values start to grow. For lower frequencies 100 – 200 kHz, the decorrelation is not as sensitive as for higher ones 300 – 400 kHz, where the obtained values start growing earlier. After the peak force is reached, the resulting decorrelation values are stabilized. The plotted curves for each sensor do not line up variously before and after the crack. Based on the diagrams, damage localization is not possible.

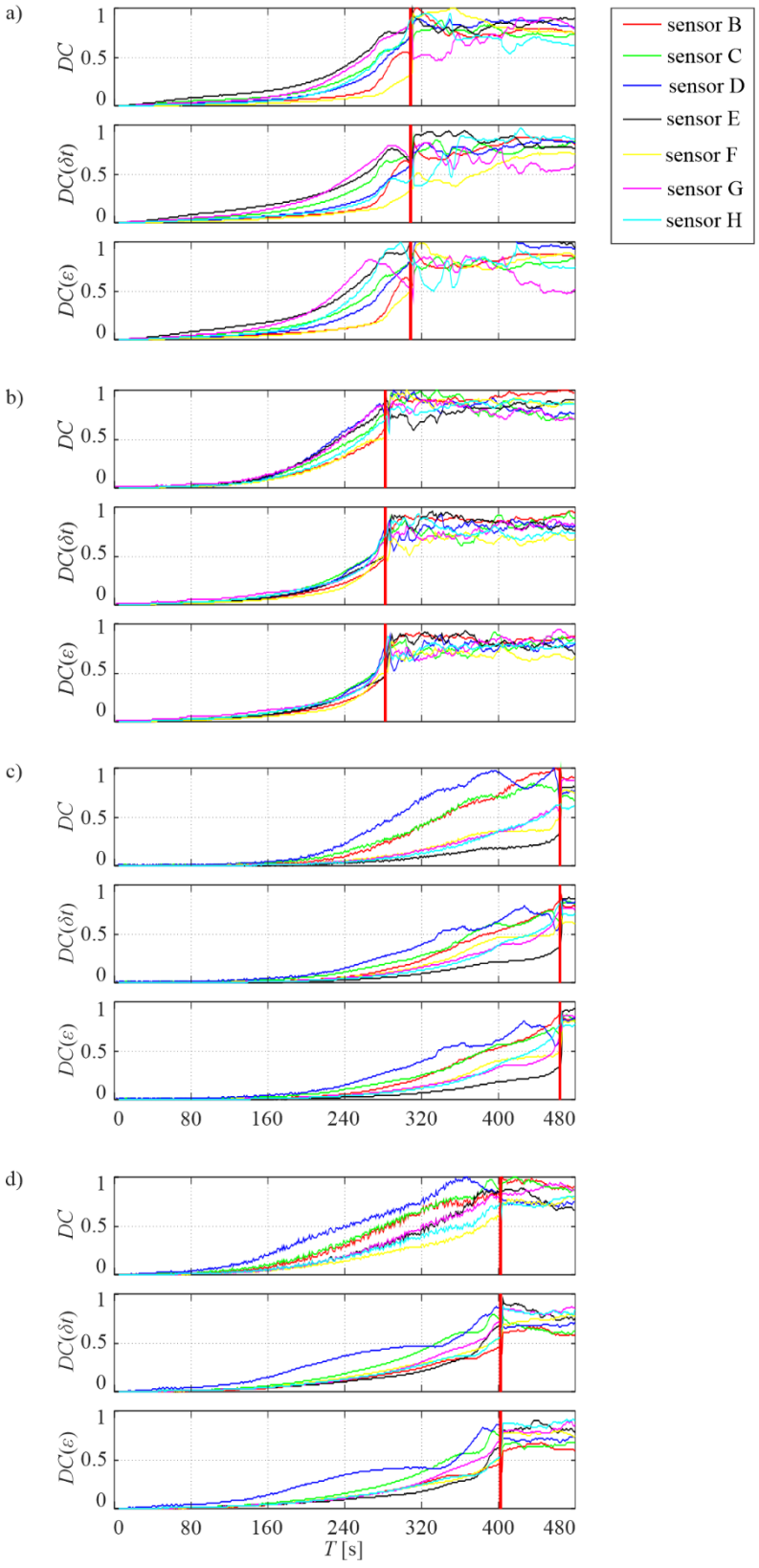

Figure 5. DC for all beams a) beam #1, b) beam #2, c) beam #3, d) beam #4.

Afterwards, maps based on *DC* diagrams from figure 5 were plotted in figure 6. The dashed lines correspond to sensor localization and the vertical, solid line refers to the load peak value. The results are presented in the time domain. It can be seen, that the results obtained from the expanded CWI methods include more information, especially after reaching peak force. Based on the plotted maps, it is difficult to localize the damage, especially at the lower frequencies of 100 – 200 kHz. At higher frequencies of 300 – 400 kHz, a clear concentration of values was obtained before the maximum force was reached at sensor D.

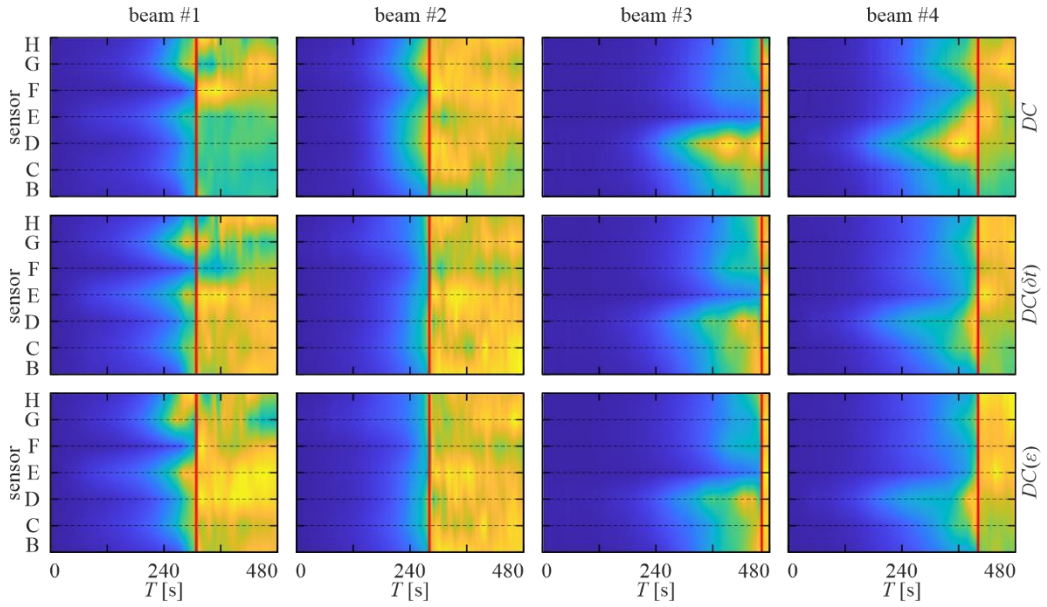

Figure 6. Maps of DC for beams #1 - #4.

Finally, an attempt to crack localization was made. Maps of DC, translation (δt) and stretching (ε) coefficients were plotted to better visualize the changes over time. The normalized absolute values of selected coefficients are presented. Figure 7 shows the results of localization for all beams. The vertical axis indicates the time of the experiment, and the horizontal axis is the distance on the beam. The vertical dashed lines refer to individual sensors, and the horizontal solid line indicates the time of occurrence of the maximum force. For each beam, a photograph of the backside with marked sensors and the location of the crack was prepared. The front side photograph was made based on DIC measurements. For each beam, the crack appearance was achieved using major strain calculations. The presented DIC images show the state after reaching the maximum force. The DIC-based strain map in figure 7 is shown in a mirror view to match both sides of the beam.

The computational values obtained from the experiment were compared with the actual location of failure. It can be observed that the behaviour of the crack is different on both sides of the beams. It makes coda imaging difficult and affects the obtained localization results. It can be seen that visualizations using translation and stretching coefficients allow better identification of the location of damage, especially for higher frequencies 300 – 400 kHz. DC maps for the classical approach contain more disorganized information, which disturbs the clarity of the results. As the frequency increases, the visualizations become more exact. For translation and stretch maps, there is a clear concentration of values in sensors in the vicinity of the crack (before and after it). Based on the results, the location of the damage can be determined.

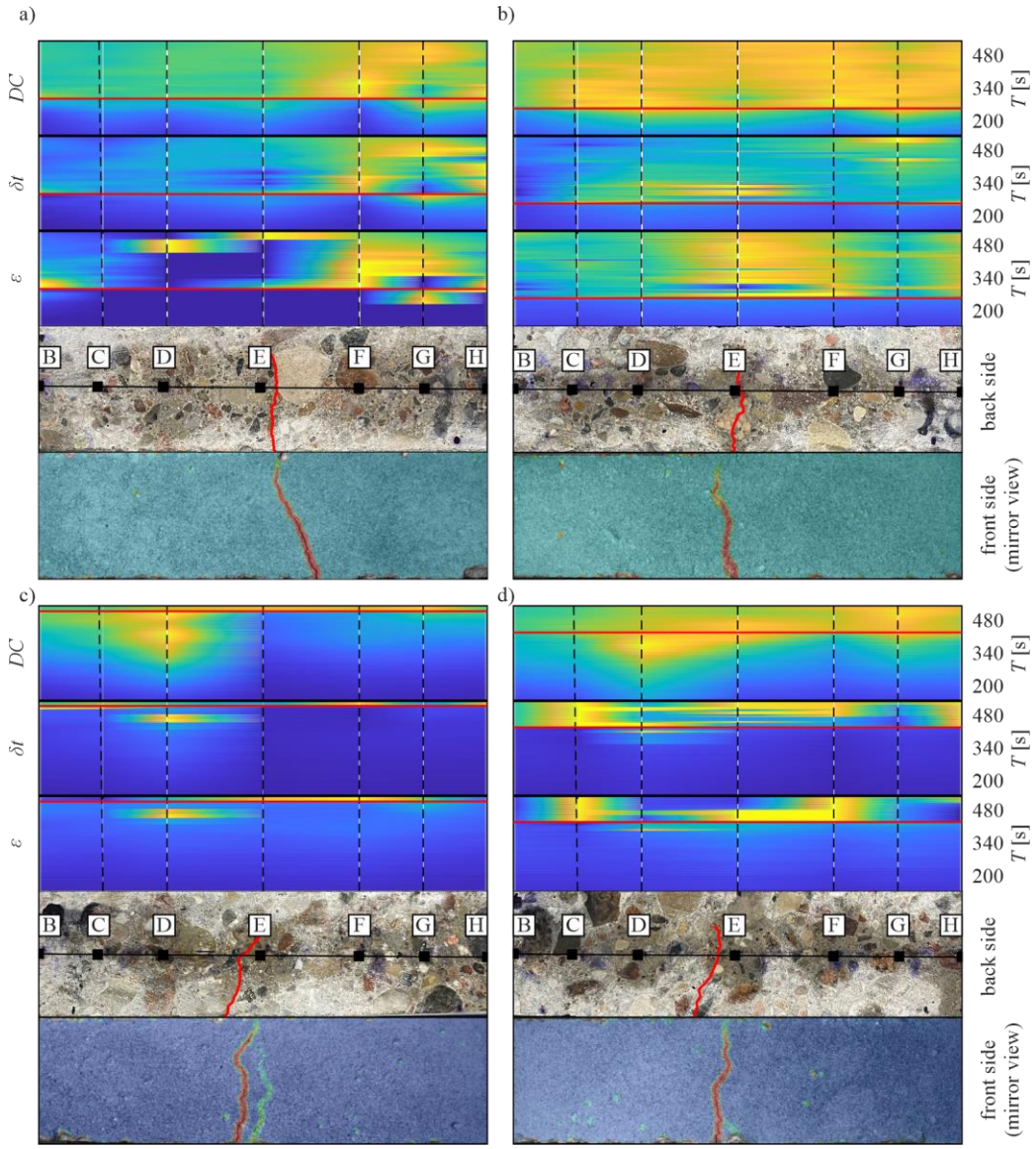

Figure 7. Detection of crack, *DC*, δt and ε maps for beams #1 - #4.

4. Conclusions

In this paper, the fracture process of concrete beams was characterized using ultrasonic tests and the coda wave interferometry method. It has been shown that the CWI method can be useful for structure monitoring and damage detection. The frequency influence on obtained results had been investigated.

First of all, ultrasonic tests made it possible to assess the condition of the structure. The visual method showed the exact position of the crack on the surface of the samples. The applied signal processing methods, based on the coda wave interferometry algorithm, gave additional information on the internal condition of the tested objects.

It was noted that the used frequency has a direct effect on CWI, and an improvement in the obtained results with its increase is reached. The higher the frequency, the coda appears in a shorter time window and there is a longer tail of noise with useless information in the signal. The higher frequencies give more accurate information about the actual state of the structure. They are more sensitive and make it possible to detect changes in an earlier phase of loading. In addition, the use of

a more complex algorithm of CWI, including translation and stretching, allowed better localization of the resulting damage.

Summarizing, the achieved results highlighted the limitations associated with the proposed ultrasonic wave-based technique with the coda wave interferometry. The presented approach allowed the selection of appropriate frequencies and highlighted the advantages of the use of a more complex method with translation or stretching. Further works will be focused on the improvement of the localization method, for example by using a sensor grid. A different spacing of sensors may allow the establishment of a planar localizer.

Acknowledgements
The wpork was funded by National Science Centre, Poland, under project no. 2019/35/B/ST8/01905.

References
[1] Zhao M Nie Z Wang K Liu P and Zhang X 2019 *Ultrasonics* **97** 1–10
[2] Deraemaeker A and Dumoulin C 2019 *Constr. Build. Mater.* **194** 42–50
[3] Chakraborty J Katunin A Klikowicz P and Salamak M 2019 *Sensors (Switzerland)* **19** 1–22
[4] Lin S Shams S Choi H and Azari H 2018 *NDT E Int.* **98** 101–9
[5] Snieder R 2006 *Pure Appl. Geophys.* **163** 455–73
[6] Zhong B and Zhu J 2022 *Appl. Sci.* **12**
[7] Fröjd P and Ulriksen P 2017 *Ultrasonics* **80** 1–8
[8] Knak M Wojtczak E and Rucka M 2023 *Bull. Pol. Acad. Sci. Tech. Sci.* 1–7
[9] Niederleithinger E Wang X Herbrand M and Müller M 2018 *Sensors (Switzerland)* **18**
[10] Wojtczak E Rucka M and Skarżyński Ł 2022 *NDT E Int.* **126**
[11] Rucka M Wojtczak E Knak M and Kurpińska M 2021 *Constr. Build. Mater.* **280**
[12] Li X Chen X Jivkov A P and Hu J 2021 *Struct. Control Heal. Monit.* **28** 1–21
[13] Meng S Shi Z Niu Y Zheng H and Xia C 2023 *Constr. Build. Mater.* **376** 131053
[14] Li S Chen X and Guo S 2020 *KSCE J. Civ. Eng.* **24** 2435–48